Chemistry–A European Journal
Research Article
doi.org/10.1002/chem.202200942
Chemistry Europe
European Chemical Societies Publishing
www.chemeurj.org

Relevance of Palladium to Radiopharmaceutical Development Considering Enhanced Coordination Properties of TE1PA

Julie Pineau,[a] Luís M. P. Lima,[b] Carlos Platas-Iglesias,[c] Jan Rijn Zeevaart,[d] Cathryn H. S. Driver,*[d] Nathalie Le Bris,*[a] and Raphaël Tripier*[a]

Abstract: The limited use of palladium-103 and -109 radionuclides for molecular radiotherapy is surely due to the lack of appropriate ligands capable of fulfilling all criteria required for application in nuclear medicine. Furthermore, the thermodynamic properties of these complexes in solution remain difficult to establish. The challenge is compounded when considering that radiolabeling of compounds for translation to clinical trials requires fast complexation. Thus, the coordination of Pd(II) and $^{103/109}$Pd-nuclides is a huge challenge in terms of molecular design and physicochemical characterization. Herein, we report a comprehensive study highlighting **TE1PA**, a monopicolinate cyclam – already established in nuclear imaging with ^{64}Cu-PET (positron emission tomography) imaging tracers – as a highly relevant chelator for natural Pd and subsequently ^{109}Pd-nuclide. The structural, thermodynamic, kinetic and radiolabeling studies of Pd(II) with **TE1PA**, as well as the comparison of this complex with three structurally related derivatives, support palladium-**TE1PA** radiopharmaceuticals as leading candidates for targeted nuclear medicine.

Introduction

Palladium(II) is recognized as a cation of interest in medicine since the 1960s when its antitumor properties, similar to those of platinum(II), were explored.[1] In 1979, antiviral, antifungal and antimicrobial properties of Pd(II) compounds were reported by Graham and Williams.[2] Nowadays, several Pd(II)-based drugs or therapeutic agents are used in more sophisticated techniques, such as targeted photodynamic therapy for localized cancer treatment.[3]

In nuclear medicine, palladium radioisotopes were first used in the early 1970s. ^{109}Pd-based molecules were described for the control of homograft rejection,[4] and ^{103}Pd-metal was introduced in 1987 as implanted seeds for brachytherapy.[5] Despite these early applications, further developments have remained very limited. However, these radiometals deserve special attention in therapy on account of their radiophysical characteristics, given the current needs for relevant radiopharmaceuticals. ^{103}Pd- and ^{109}Pd-radionuclides have half-lives ($t_{1/2}$) of 17 days and 13.7 h, respectively. Palladium-103 decays by electron capture (EC) and Auger electron (AE) emissions to the ^{103m}Rh-daughter ($t_{1/2}$ = 56 min), which is another AE emitter that decays to stable Rh.[6] It is commercially available via cyclotron production as a high specific activity, no-carrier added product.[7] ^{109}Pd-nuclide decays by β^- particle emission ($E_{\beta(max)}$ = 1.12 MeV, 100% yield) to the daughter nuclide, silver-109 m ($t_{1/2}$ = 39.6 s), which in turn emits a photon (88 keV, 3.6% yield) accompanied by conversion electron emissions and AE emissions leading to the stable ^{109}Ag-nuclide.[8] Palladium-109 is easily produced with moderate specific activity from an isotopically enriched ^{108}Pd-target in a neutron reactor.[8]

The optimal use of therapeutic radiopharmaceuticals requires combination with a radiodiagnostic agent that allows for patient disease staging and treatment monitoring. Diagnostic radiotracers employ radionuclides, commonly metallic elements, with emissions that can be detected by specialized cameras and allow for disease imaging. These emissions include positrons (β^+) and photons (γ) for PET (positron emission

[a] J. Pineau, Dr. N. Le Bris, Prof. R. Tripier
Univ Brest, UMR CNRS 6521 CEMCA
6 avenue Victor le Gorgeu, 29238 Brest (France)
E-mail: s:
E-mail: nathalie.lebris@univ-brest.fr
raphael.tripier@univ-brest.fr
[b] Dr. L. M. P. Lima
Instituto de Tecnologia Química e Biológica António Xavier
Universidade Nova de Lisboa
Av. da República, 2780-157 Oeiras (Portugal)
[c] Prof. C. Platas-Iglesias
Departamento de Química
Facultade de Ciencias & Centro de Investigaciones Científicas Avanzadas (CICA)
Universidade da Coruña
San Vicente de Elviña, 15071 A Coruña (Spain)
[d] Prof. J. R. Zeevaart, Dr. C. H. S. Driver
South African Nuclear Energy Corporation
Radiochemistry and PreClinical Imaging Facility
Elias Motsoaledi Street, R104 Pelindaba, North West, 0240 (South Africa)
E-mail: Cathryn.Driver@necsa.co.za

Supporting information for this article is available on the WWW under https://doi.org/10.1002/chem.202200942

tomography) and SPECT (single-photon emission computed tomography), respectively.[9]

For the development of radiopharmaceuticals utilizing metallic radionuclides, the radiometals produced in their cationic form must be complexed with a chelator that fulfills all the necessary criteria for in vivo applications. The complex formed with the radiometal should be very stable, both in terms of thermodynamic stability and kinetic inertness.[10] Moreover, the chelator must be bifunctional, in other words, besides its coordination properties, it must have an additional functional group suitable for conjugation to targeting biomolecules without compromising complex stability.[11] The perfect match between the metallic cation and the design of the chelator is therefore the crucial factor for achieving the desired physic-chemical properties of the complex.

Given the wide range of radionuclides of interest for medical applications, a large panel of chelating agents have been reported in the literature.[12] The current quest is to find versatile chelating agents capable of complexing a theranostic pair, meaning two radionuclides suitable for both diagnosis and therapy.[13]

Radionuclides for therapy, such as lutetium-177 or yttrium-90 (β^-), have been successfully paired with gallium-68 (β^+) for PET imaging.[14] However this pairing is not ideal as the corresponding half-lives of the radionuclides are not well matched (6.7 days for ^{177}Lu, 2.7 days for ^{90}Y vs. 68 min for ^{68}Ga-nuclide) and their coordination properties differ considerably, with typical coordination numbers of 8–10 for Lu(III) and Y(III) vs. 6 for Ga(III). In addition to these heterotopic pairs, a few pairs of homotopic elements, such as ^{64}Cu/^{67}Cu-isotopes, are of an increasing interest.[15] The β^+ emitter, copper-64 ($t_{1/2}$ = 12.7 h) is produced worldwide for PET imaging in preclinical and clinical trials. The therapeutic partner, copper-67 ($t_{1/2}$ = 61.8 h), is a β^- emitter but its rather low emission energy ($E_{\beta-(max)}$ = 0.577 MeV) might limit its treatment potential; therefore, finding alternative radionuclides with suitable therapeutic emissions to be paired with copper-64 would be highly beneficial.

While presenting interesting properties, palladium radioisotopes have been sparsely used in the context of radiopharmaceutical development, and only a few ligands such as DTPA[16] and porphyrins were explored.[17] The most reasonable explanation for this is that the palladium coordination chemistry does not match the chelators considered as gold standards in nuclear medicine, namely DOTA (1,4,7,10-tetraazacyclododecane-1,4,7,10-tetraacetic acid) and NOTA (1,4,7-triazacyclononane-1,4,7-triacetic acid) derivatives. Palladium, a second-row transition metal with the electronic configuration [Kr]4d^{10}, mainly forms four-coordinate complexes with a square-planar geometry not compatible with the previous ligands.[18]

Many ligands have already been proposed for Pd(II) complexation,[19] but examples providing highly stable and inert complexes[20] are very rare. This is likely because many applications do not require such stringent properties (i.e. catalysts). A recent review showed that open chain polyamines and macrocyclic polyamines such as cyclam (1,4,8,11-tetraazacyclotetradecane) have advantageous properties for Pd(II) coordination.[21] Cyclam is a well-known scaffold forming highly stable and inert complexes with small transition metal ions such as Ni(II), Co(II) or Cu(II).[22] Furthermore, cyclam forms a square-planar complex with Pd(II) with an extremely high stability constant (log K = 56.9).[23]

Our group developed the monopicolinate cyclam derivative **TE1PA**, which exhibits improved properties for ^{64}Cu-immuno-PET imaging in terms of radiolabeling yield, conjugation to antibody, biodistribution, and pharmacokinetics as compared to those of DOTA and NOTA derivatives.[24,25] Thus, we sought to investigate the coordination of **TE1PA** with natural Pd and palladium-109 to assess whether this chelator could be used for the coordination of both Cu(II) and Pd(II), and potentially used for the development of new radiopharmaceuticals based on the ^{64}Cu/^{103}Pd- or ^{64}Cu/^{109}Pd-theranostic pairs. For a better understanding of the different factors that drive complexation, three other ligands (Figure 1) were studied in addition to **TE1PA**: **cyclam**, **TE1Bn** (benzyl cyclam) and **TE1Py** (pyridylmethyl cyclam).

Results and Discussion

Synthesis and solid-state studies

TE1Py was obtained following a new synthetic route starting from the easily synthesized triBoc-**cyclam** (see procedure in Supporting Information, Scheme S1 and Figures S1-S4). All other chelators were obtained using established syntheses methods (see Supporting Information). The synthesis of the Pd(II) complexes was performed in refluxing aqueous solution using Na_2PdCl_4 over 16 h at pH 4 (to avoid metal hydroxide precipitation). All complexes were obtained as yellowish powders in yields of around 60% following purification (see procedures in Supporting Information and Figure S5 to S14).

The structures of [Pd(**TE1Bn**)]$^{2+}$ and [Pd(**TE1PA**)]$^{+}$ obtained by X-ray diffraction are shown in Figures 2 and 3, while those of Pd(**cyclam**)]$^{2+}$and [Pd(**TE1Py**)]$^{2+}$ are presented in the Supporting Information (Figures S15-16). Selected bond lengths and angles for all complexes are given in Table 1 (additional data in Tables S1 to S5). Crystals of [Pd(**cyclam**)]$(Cl)_2{\cdot}6H_2O$ suitable for X-ray diffraction studies were obtained by slow evaporation from aqueous solution at pH 7. The structure is very similar to those of [Pd(**cyclam**)]$(ClO_4)_2$ and [Pd(**cyclam**)]$(Cl)_2$ reported previously,[26,27] though with slightly different bond distances and angles. The structure evidences square-planar coordination with the Pd(II) ion located in the plane defined by the four

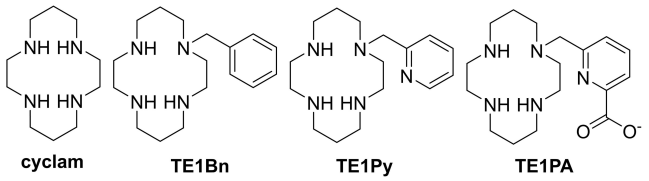

Figure 1. Ligands discussed in this study.

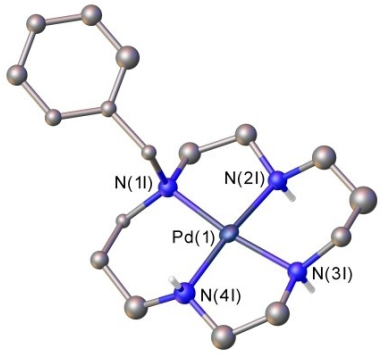

Figure 2. ORTEP diagram of the crystal structure of [Pd(**TE1Bn**)]$^{2+}$ cation plotted at 30% of ellipsoids probability.

nitrogen atoms. The hydrogen atoms of the two amino functions separated by a propylene bridge point to the same side of the N_4 plane, and opposite to the other two hydrogen atoms, resulting in a *trans*-III configuration according to Bosnich's nomenclature.[28] The two six-membered chelate rings adopt chair conformations.

Crystals of [Pd(**TE1Bn**)](PdCl$_4$) were obtained by slow evaporation under heating of a solution of the complex in DMSO. The structure resembles that of the parent unsubstituted complex, [Pd(**cyclam**)]$^{2+}$, in that a *trans*-III configuration is obtained with minimal distortion from a square-planar geometry (Figure 2). The presence of the benzyl group on N(1I) does not significantly affect the Pd(1)–N(1I) bond length value of 2.012(19) Å, which is similar to the Pd-NH bonds (Table 1). The N(4I)–Pd(1)–N(1I) angle [98.0(7)°] involving the six-membered chelate ring bearing the benzyl group is considerably more open than the N(2I)–Pd(1)–N(3I) angle [86.8(6)°]. In the five-membered chelate rings, N(1I)–Pd(1)–N(2I) and N(4I)–Pd(1)–N-N(3I) angles are respectively equal to 86.0(7)° and 89.4(7)°. These N–Pd–N angles show similar tendencies to the two differently regiosubstituted *N,N'*-dibenzyl-cyclam palladium complexes described by Turner.[29]

Crystals of [Pd(**TE1Py**)](PdCl$_4$) were obtained by slow evaporation of an aqueous solution of the complex at room temperature. While the crystal structure had a poor quality (Figure S16), it revealed a *trans*-III configuration similar to that obtained for the Pd-**TE1Bn** complex; the bond lengths and angles have to be considered cautiously because of the low resolution. The substitution of the benzyl group of **TE1Bn** by a

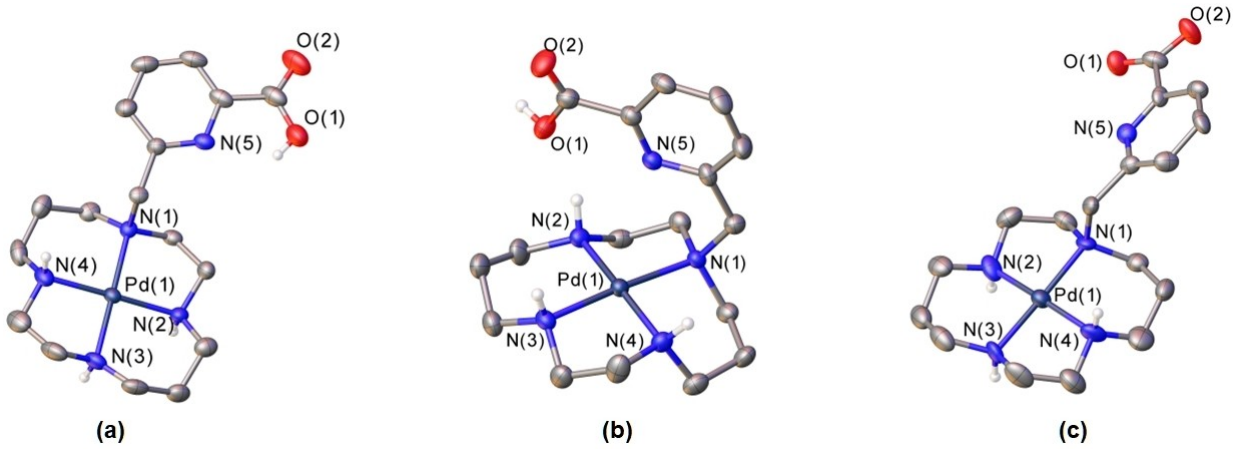

Figure 3. ORTEP diagrams of the crystal structures of (**a**) [Pd(H**TE1PA**)]$^{2+}$ obtained from a 5 M HCl solution, (**b**) [Pd(H**TE1PA**)]$^{2+}$ at pH 3.5 and (**c**) [Pd(**TE1PA**)]$^{+}$ at pH 7, plotted at 30% of ellipsoids probability.

Table 1. Selected bond lengths (Å) and angles (°) for all complexes.

	[Pd(**cyclam**)]$^{2+}$	[Pd(**TE1Bn**)]$^{2+}$	[Pd(**TE1Py**)]$^{2+}$	[Pd(H**TE1PA**]$^{+}$ 5 M HCl	[Pd(H**TE1PA**)]$^{+}$ pH 3.5	[Pd(**TE1PA**)]$^{2+}$ pH 7
Configuration	*trans*-III	*trans*-III	*trans*-III	*trans*-III	*trans*-I	*trans*-III
Pd(1)–N(1)	2.039(6)	2.012(19)	2.074[a]	2.059(5)	2.080(5)	2.009(10)
Pd(1)–N(2)	2.031(5)	1.978(15)	2.024[a]	2.044(5)	2.035(5)	1.998(12)
Pd(1)–N(3)	–	2.036(16)	2.042[a]	2.057(5)	2.038(5)	2.007(10)
Pd(1)–N(4)	–	1.997(16)	2.040[a]	2.046(6)	2.045(5)	2.050(12)
Pd(1)–N(5)	–	–	–	5.015	3.066	5.002
N(2)–H(2)–O(1)	–	–	–	–	2.18(2)	–
N(1)–Pd(1)–N(2)	85.3(3)	86.0(7)	84.33[a]	85.49(18)	84.98(19)	84.2(5)
N(2)–Pd(1)–N(3)	94.7(3)	86.8(6)	94.54[a]	95.0(2)	96.8(2)	95.8(4)
N(3)–Pd(1)–N(4)	–	89.4(7)	84.31[a]	85.2(2)	84.8(2)	84.5(5)
N(4)–Pd(1)–N(1)	–	98.0(7)	96.87[a]	94.4(2)	93.2(2)	95.6(4)

[a] structure of poor quality and low resolution

pyridylmethyl group in **TE1Py** does not significantly affect the bond lengths of the Pd(II) coordination sphere, but has a greater impact on the various bond angles. The values of the N(1)–Pd(1)–N(2) and N(3)–Pd(1)–N(4) angles, corresponding to the five-membered chelate rings, are below 85°, while the N(2)–Pd(1)–N(3) and N(4)–Pd(1)–N(1) angles are above 94°.

Three different crystal structures were obtained for the **TE1PA** complex by evaporation of aqueous solutions at different pH values (pH < 0, 3.5 and 7) (Figure 3). In each case, the Pd(II) ion is four-coordinated by the nitrogen atoms of the cyclam core. The nitrogen atom of the picolinate unit is not bound to palladium, regardless of whether the carboxylate function is protonated or not. The structure of [Pd(H**TE1PA**)](PdCl$_4$) obtained from a 5 M HCl aqueous solution shows a *trans*-III configuration, while interestingly those obtained from an aqueous solution at pH 3.5 reveal a *trans*-I configuration. Crystals of [Pd(**TE1PA**)](ClO$_4$)·2H$_2$O obtained at pH 7 (by adjusting the pH with NaOH) after addition of NaClO$_4$ again indicate a structure with the *trans*-III configuration. The Pd–N bond lengths of the *trans*-III complex obtained in 5 M HCl are between 2.044(5)-2.059(5) Å, while those of the *trans*-III complex isolated at pH 7 are slightly shorter, ranging from 1.998(12) to 2.050(12) Å. The Pd(1)–N(1) bond, which involves the picolinate substituent, shows very different distances of 2.059(5) (5 M HCl) against 2.009(10) Å (complex at pH 7). A similar situation is observed for the Pd(1)–N(2) and Pd(1)–N(3) bonds, while the Pd(1)–N(4) distances are virtually identical. For the *trans*-I complex, the Pd(1)–N(1) distance of 2.080(5) Å is much longer than the Pd-NH distances of Pd(1)–N(2) at 2.035(5) Å, Pd(1)–N(3) at 2.038(5) Å, and Pd(1)–N(4) at 2.045(5) Å (Table 1), but also much longer than the Pd(1)–N(1) distance in the *trans*-III complex. For both the *trans*-III and *trans*-I configurations, the angles characterizing the five-membered chelate rings (N(1)–Pd(1)–N(2) and N(3)–Pd(1)–N(4), < 86°) are lower than those involving six-membered chelate rings (N(2)–Pd(1)–N(3) and N(4)–Pd(1)–N(1), > 93°). In both *trans*-III complexes, the distance between the metal center and the nitrogen atom of the pyridyl unit N(5) is > 5 Å, since the picolinate arm is orientated away from the central plane of the cyclam unit. On the contrary, in the *trans*-I configuration the protonated picolinate arm points towards the cyclam core, generating an intramolecular hydrogen bonding interaction between one NH group of the macrocycle and one oxygen atom of the carboxylic acid group (N(2)–H(2)····O(1), 2.18(2) Å).

Structural studies in solution

The ^{1}H and ^{13}C NMR spectra of [Pd(**cyclam**)]$^{2+}$ were performed in D$_2$O or in methanol-d4 (Figures S5-6). The ^{13}C NMR spectrum surprisingly indicated two series of peaks not visible in the ^{1}H NMR spectrum. The proportion of the minor species was dependent on the solvent, ranging from 10% in methanol-d4 to about 30% in D$_2$O irrespective of the pD (4 and 7). Sadler and coll. reported in 2004[27] that only one species with the *trans*-III configuration existed in solution, suggesting that the presence of a second species, such as the *trans*-I configuration, is possible depending on experimental conditions. DFT calculations indeed predict that the *trans*-I and *trans*-III configurations are significantly more stable than *trans*-II and *cis*-V (Table S6). The relative free energies calculated showed that the *trans*-III isomer is favored by only 2.5 kcal mol^{-1} over *trans*-I. Calculations of the ^{13}C NMR shifts using relativistic DFT calculations allowed for assignment of the major species present in solution to the *trans*-III isomer, in agreement with the relative energies and the X-ray structures (Table S7).

For the [Pd(**TE1Bn**)]$^{2+}$ complex, the NMR study performed in DMSO-d6 for solubility reasons, exhibited one main series of peaks in both ^{1}H and ^{13}C NMR spectra (Figure S8). However, one other series of peaks corresponding to the minor isomer was also observed. This complex has already been described by Lindoy and co-workers,[29] but without any details concerning the species present in solution. However, the NMR spectra clearly indicated more peaks than expected for one single isomer. The relative energies calculated for [Pd(**TE1Bn**)]$^{2+}$ by DFT are very sensitive to the inclusion of explicit second-sphere water molecules. Calculations performed on the [Pd(**TE1Bn**)](PdCl$_4$)·2H$_2$O system suggest that the *trans*-III isomer is the most stable configuration, roughly by 2 kcal mol^{-1} with respect to the *trans*-I configuration. Thus, most likely both *trans*-III and *trans*-I isomers are present in solution, though an unambiguous assignment of the major species present in solution cannot be performed on the grounds of our NMR data. The NMR spectra of [Pd(**TE1Py**)]$^{2+}$ in D$_2$O (Figure S10) are very similar to those of the [Pd(**TE1Bn**)]$^{2+}$ complex, with one main species most likely corresponding to the *trans*-III configuration.

For [Pd(**TE1PA**)]$^{+}$, spectra recorded in D$_2$O at pD 7 (Figure S12) displayed two sets of signals with similar populations, assigned to the *trans*-I and *trans*-III configurations. Adjustment of the pD to 4 in the same sample did not change the proportions of the two populations (Figure S13). The DFT calculations revealed rather similar energies for these two isomers, while the *trans*-II and *cis*-V isomers are characterized by higher energies (Table S6). A summary of the different configurations obtained in solution for the studied Pd(II) complexes is given in Table S8.

Thermodynamic studies

Cyclam is known to form a Pd(II) complex displaying outstandingly high thermodynamic stability,[23] but to our knowledge this property has only been investigated in one other cyclam derivative, tetra(2-hydroxyethyl) cyclam.[30] The reason for this is the notorious difficulties in studying Pd(II) complexation in aqueous media, namely: the marked tendency of this metal cation to form insoluble hydrolysis species in all but the most acidic pH ranges, the frequently high stability of its polyamine complexes, and a predisposition to display slow complexation kinetics with structurally rigid ligands. In order to enable a detailed study of the complexation properties of Pd(II) with monosubstituted cyclam derivatives, a combination of UV spectrophotometry and potentiometry performed in aqueous medium at 25 °C was used. To overcome the expected high

values of the formation constants for the complexes, the UV titrations were run in a very acidic solution (pH = 0–1.5) at a 1.0 M concentration of (K,H)Cl electrolyte. In such low pH conditions, Pd(II) complexation could be observed for both **TE1PA** and **TE1Py**. Fitting of the UV spectroscopy data then allowed for determination of the formation constant for the protonated species $[Pd(H_2\mathbf{TE1PA})]^{3+}$ or $[Pd(H\mathbf{TE1Py})]^{3+}$ with subsequent establishment of the remaining equilibrium constants for the existing species (constants were fitted to the potentiometric titration of the corresponding system). No formation constant for any complex species of **TE1Bn** could be determined as the complex appears to be fully formed under the used experimental conditions. However, from the UV data it can be speculated that its log *K* value should be higher than ca. 43. The ligand protonation equilibria were studied by potentiometry in 1.0 M KCl aqueous medium, as were the protonation equilibria of the Pd(II) complexes since these are fully formed at pH ≥ 2.0. The protonation and complexation constants are presented in Table 2 (and Table S9), while species distribution diagrams are presented in Figures S17 and S18.

The protonation constants of the ligands display the usual pattern found for cyclam derivatives of two basic protonation centers while the remaining ones are more acidic. A previously observed feature, consistent with **cyclam**, is that both **TE1Py** and **TE1Bn** show the uncommon inversion of values for two acidic protonation centers where the third constant is lower than the fourth. This feature has been attributed to the increased strain exhibited upon addition of the third proton to the cyclam skeleton.[31] For the Pd(II) complexes, using the previously UV-determined formation constants to fit the potentiometric data, it was found that **TE1PA** shows a very high stability constant (log K_{ML} = 38.4), while **TE1Py** displays an even higher constant (log K_{ML} = 42.6). Both values are much higher than for the tetra(2-hydroxyethyl) cyclam derivative (log K_{ML} = 18.32),[30] despite still being significantly lower than the value estimated for cyclam itself (log K_{ML} = 56.9).[23]

Inertness

The slow dissociation of the complexes is probably the most important feature to be evaluated for the selection of medically relevant compounds. The acid-assisted dissociations of the **cyclam** and **TE1PA** complexes were studied in acidic aqueous solutions. The dissociation was monitored using ^{1}H NMR by following the changes of the complexes at 90 °C in 5 M DCl. The unchanged spectra (Figure S19-S20) unambiguously showed absolutely no evolution of the structures even after five months incubation with constant stirring. This confirms the perfect matching of the cyclam core with Pd(II), and that the presence of the picolinate pendant in **TE1PA**, even if not involved in the metal coordination scheme, does not compromise kinetic inertness.

Table 2. Stepwise protonation (log K_{HiL}) and Pd(II) complexation (log K_{PdHiL}) constants for **TE1PA**, **TE1Py** and **TE1Bn** determined at 25 °C in 1.0 M KCl aqueous solution.

Equilibrium reaction[a]	TE1PA	TE1Py	TE1Bn
$L + H^+ \rightleftarrows HL$	11.13(1)	11.50(1)	11.31(1)
$HL + H^+ \rightleftarrows H_2L$	10.06(1)	10.39(1)	9.39(1)
$H_2L + H^+ \rightleftarrows H_3L$	3.05(2)	2.65(1)	2.21(1)
$H_3L + H^+ \rightleftarrows H_4L$	2.28(3)	2.83(1)	2.89(2)
$H_4L + H^+ \rightleftarrows H_5L$	1.69(8)	–	–
$Pd^{2+} + L \rightleftarrows PdL$	38.4(1)	42.6(1)	>43
$PdL + H^+ \rightleftarrows PdHL$	2.9(1)	1.6(1)	–
$PdHL + H^+ \rightleftarrows PdH_2L$	1.8(1)	–	–

[a] Charges are omitted for clarity.

^{109}Pd Radiolabeling

Considering the very high stability constants of the Pd(II)-**cyclam** derivative complexes and their inertness in acidic medium, all cyclam derivatives were studied for complexation of the ^{109}Pd-radioisotope (see procedure in Supporting Information). The aim was to compare the macrocycles, and specifically **TE1PA** and **cyclam**, in terms of their ^{109}Pd-labelling efficiency (the kinetic process of complexation) and inertness under radiolabeling conditions for potential application in developing new palladium-based radiopharmaceuticals.

The ^{109}Pd-radionuclide was produced with a specific activity of 2.9 GBq/mg (78 mCi/mg) from a 94% enriched ^{108}Pd-target following high-flux neutron beam irradiation. After the precipitation and separation of Ag-radionuclide impurities from the processed $[^{109}Pd][PdCl_4^{2-}]$ solution, gamma ray spectroscopy (88 keV (gamma from ^{109m}Ag-daughter nuclide), 311, 413, 602, 636, 647, 781 keV) indicated a radionuclidic purity >99.9% with a radiochemical yield of 90%. While palladium-109 is easily accessible, the disadvantage is that the molar activity of the obtained radionuclide is only moderate. In the long run, this might limit biological application, however it is more than sufficient for evaluation of chelator complexation properties.

In order to compare the efficiency of the different chelators for ^{109}Pd-complexation, the radiolabeling reactions were performed in 0.1 M NH_4OAc at different pH values (pH 3.5, 7 and 8.5), two temperatures (25 and 90 °C), and different reaction times (10 and 30 min). An approximate two-fold excess molar ratio of chelator:metal (2–2.5 : 1)(based on starting mass of irradiated target and subsequent approximate concentration of ^{109}Pd-solution) was used to ensure maximum metal complexation. The reactions were then analyzed by radio-HPLC (Figure S21) to determine the radiolabeling efficiency (% LE).

The radiometal complexation for all chelators was very good (>90% LE) at pH 3.5 and 90 °C over 30 min. The relatively long reaction time at this temperature provided enough energy to activate metal-chelator bond formation and to overcome the kinetic process of complexation to all four ligands. For comparison purposes, the radiolabeling efficiencies were evaluated at different temperatures over the shorter reaction time of 10 min. These results are presented in Figure 4, Figure S22 and Table S10.

With 99% LE at 90 °C and 96% at room temperature within 10 min, **TE1PA** clearly presented the best efficiency for complexation of ^{109}Pd-nuclide among the four chelators. While heating generally improved the radiolabeling efficiency, the chart in Figure 4 clearly demonstrates that the functionalization of the cyclam backbone accelerates the radiolabeling, especially looking at the results at room temperature. Indeed, the poor LE obtained for **cyclam** is evidence of slow complexation kinetics, particularly at short radiolabeling times, and indicates that longer times (> 30 min) and high temperatures are required to improve complexation (≥ 90% LE). The differences between LEs of **TE1Bn**, **TE1Py**, and **TE1PA** at 90 °C are not very significant. However, these chelators show rather different performances at room temperature (96% for **TE1PA** vs. 78% and 70% for **TE1Py** and **TE1Bn**, respectively). Most likely, the picolinate moiety at pH 3.5 is rather efficient in chelating Pd(II) close to the macrocyclic cavity, perhaps assisted by the intramolecular hydrogen bond observed in the X-ray structure (N(2)–H-(2)···O(1)). This intermediate can then evolve to the final complex upon coordination of Pd(II) to the N atoms of the macrocycle. The results for labelling experiments performed at other pH values (7.0 and 8.5, Figures S23-S25) evidence a noticeable drop in radiolabeling efficiency for all chelators with respect to pH 3.5, except for **TE1PA**. Under these radiolabeling conditions, the [^{109}Pd][Pd(**TE1PA**)]$^{+}$ complex is formed with a very high radiolabeling yield as compared to the other chelators, (LE > 85% for **TE1PA**, and < 40% for **cyclam**, **TE1Bn** and **TE1Py**; 90 °C, 30 min). Even at a pH of 8.5 at room temperature with a short reaction time, the LE of **TE1PA** stay moderate (35%) as compared to the LE of the other chelators that falls to values < 5%. Interestingly, the ^{109}Pd-labelling reactions completed in a 0.01 M PBS buffer (pH 6.5–7.0) for 10 min at 25 °C or 90 °C resulted in very high LEs (≥ 95%) for all chelators, except for cyclam at room temperature (38%) (Figure S25). The higher labelling efficiencies are most likely as a result of the PBS buffer preventing extensive precipitation of palladium hydroxide, while the conformational rearrangement necessary for cyclam to accommodate the metal is not kinetically favored and the LE is therefore limited at lower temperatures.

To further investigate and compare the radiolabeled complex inertness with regard to transchelation, an EDTA challenge was performed under physiological pH conditions in PBS buffer (0.01 M, pH 7). **TE1PA** and **cyclam** were radiolabeled with palladium-109 in PBS buffer at 90 °C to obtain maximum radionuclide complexation (> 98%) and then challenged by an EDTA solution (1000 eq) at room temperature. Transchelation to EDTA was then monitored by radio-HPLC over 24 h (Figure 5).

Not much transchelation was observed at the early time points with the behavior of both radio-complexes being quite similar (only 2–3% loss of the radiometal). However, a significant improvement in inertness of [^{109}Pd][Pd(TE1PA)]$^{+}$ over [^{109}Pd][Pd(**cyclam**)]$^{2+}$ is observed after 24 h at room temperature, ultimately demonstrating the enhanced properties of the picolinate derivative.

Conclusion

Considering their radiophysical properties, both ^{109}Pd- and ^{103}Pd-isotopes are very attractive radionuclides for therapeutic purposes in nuclear medicine. Moreover, these radionuclides could be associated with β^{+}-emitters to form attractive theranostic pairs as effective solutions for the monitoring and treatment of patients with cancers. However, the progress towards this end has been hindered by the lack of efficient chelators able to comply with the required physicochemical specifications in terms of kinetics and thermodynamics. After a thorough review of the literature, macrocyclic polyamines, especially cyclam and its derivatives, appeared to be good candidates for Pd(II) complexation. Thus, cyclam-based chelators efficient for ^{64}Cu-radiolabelling, such as **TE1PA**, should also be efficient for Pd(II) coordination. The comparative study of the Pd(II) complexes obtained with **cyclam**, **TE1Bn**, **TE1Py**, and **TE1PA** clearly showed that all complexes displayed mainly the *trans*-III configuration in the solid state, but both *trans*-I and *trans*-III configurations

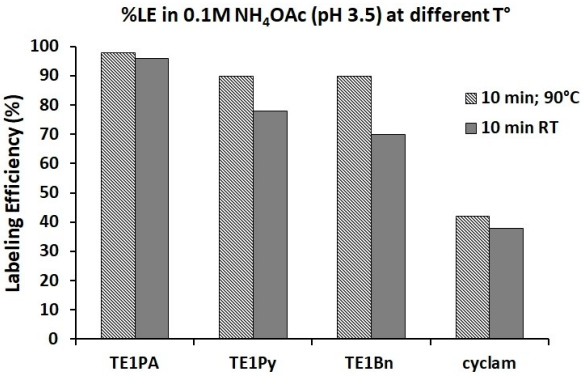

Figure 4. Comparison of ^{109}Pd-labelling of selected macrocyclic ligands at pH 3.5 in 0.1 M NH_4OAc after 10 minutes at room temperature (25 °C) and 90 °C.

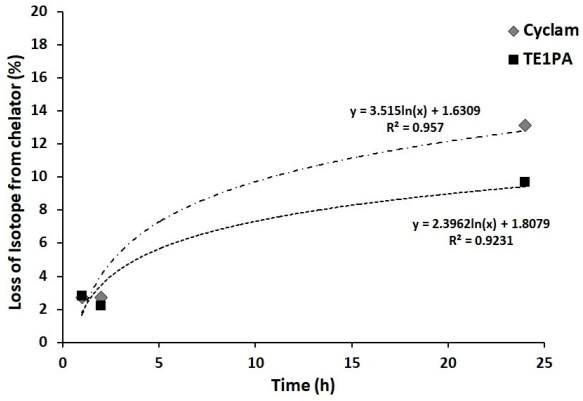

Figure 5. EDTA challenge (1000 eq) of [^{109}Pd][Pd(**TE1PA**)]$^{+}$ and [^{109}Pd][Pd-(**cyclam**)]$^{2+}$ in PBS (0.01 M, pH 7) at 25 °C over a 24 h period

were present in solution. We succeeded in implementing, to our knowledge, the first thermodynamic study combining potentiometry and UV spectroscopy that allowed measurements of the complexation constants obtained with the mono-functionalized chelators. As expected, ligand functionalization decreased the thermodynamic stability of the complexes, which nonetheless still presented extremely high stability constants (log $K_{ML} = 38.4$ for [Pd(**TE1PA**)]$^{+}$). Radiolabeling studies unambiguously showed that the presence of the picolinate pendant on the cyclam backbone improved both the ^{109}Pd-radiolabelling efficiency in mild conditions and the inertness with respect to transchelation. This paves the way for the appealing use of bifunctional **TE1PA** derivatives[25] for therapeutic purposes with Pd radioisotopes, as well as for a theranostic application when combined with copper-64 for PET imaging.

X-ray structures: Deposition Numbers 2159599 (for [Pd(**cyclam**)]$^{2+}$), 2159601 (for [Pd(**TE1Bn**)]$^{2+}$), 215602 (for [Pd(H**TE1PA**)]$^{2+}$ obtained from a 5 M HCl solution), 2159598 (for [Pd(H**TE1PA**)]$^{2+}$ at pH 3.5), 2159600 (for [Pd(**TE1PA**)]$^{+}$ at pH 7) contain the supplementary crystallographic data for this paper. These data are provided free of charge by the joint Cambridge Crystallographic Data Centre and Fachinformationszentrum Karlsruhe Access Structures service.

Acknowledgements

R.T. and N.L.B. acknowledge the Ministère de l'Enseignement Supérieur et de la Recherche and the Centre National de la Recherche Scientifique. J.P. is grateful to the Ligue contre le Cancer, the MAC-group (UBO) and the University of Cape Town for her PhD fellowship; C.H.S.D thanks the Technology Innovation Agency (TIA) seed fund implemented through the South African Nuclear Energy Corporation for financial support. C.P.-I. thanks Centro de Supercomputación de Galicia for providing access to computing facilities. L.M.P.L was financially supported by Project LISBOA-01-0145-FEDER-007660 (Microbiologia Molecular, Estrutural e Celular), funded by FEDER funds through COMPETE2020 - Programa Operacional Competitividade e Internacionalização (POCI) and by national funds through FCT - Fundação para a Ciência e a Tecnologia.

Conflict of Interest

The authors declare no conflict of interest.

Data Availability Statement

The data that support the findings of this study are available in the supplementary material of this article.

Keywords: cyclam · cyclam monopicolinate · complexation · palladium(II) · palladium-109 · radiolabeling

[1] S. Kirschner, Y.-K. Wei, D. Francis, J. G. Bergman, *J. Med. Chem.* **1966**, *9*, 369–372.
[2] R. D. Graham, D. R. Williams, *J. Inorg. Nucl. Chem.* **1979**, *41*, 1245–1249.
[3] a) M. P. M. Marques, *ISRN Spectrosc.* **2013**, 1–29; b) T. J. Carneiro, A. S. Martins, M. P. M. Marques, A. M. Gil, *Front. Oncol.* **2020**, *10*, 590970; c) Y. Vakrat-Haglili, L. Weiner, V. Brumfeld, A. Brandis, Y. Salomon, B. McIlroy, B. C. Wilson, A. Pawlak, M. Rozanowska, T. Sarna, A. Scherz, *J. Am. Chem. Soc.* **2005**, *127*, 6487–6497.
[4] a) M. Savastano, P. Arranz-Mascarós, C. Bazzicalupi, M. P. Clares, M. L. Godino-Salido, M. D. Gutiérrez-Valero, M. Inclán, A. Bianchi, E. García-España, R. Lopez-Garzón, *J. Cat.* **2017**, *353*, 239–249; b) M. Passaponti, M. Savastano, M. P. Clares, M. Inclán, A. Lavacchi, A. Bianchi, E. García-España, M. Innocenti, *Inorg. Chem.* **2018**, *57*, 14484–14488; c) M. Savastano, P. Arranz-Mascarós, M. P. Clares, R. Cuesta, M. L. Godino-Salido, L. Guijarro, M. D. Gutiérrez-Valero, M. Inclán, A. Bianchi, E. García-España, R. Lopez-Garzón, *Molecules* **2019**, *24*, 1–19.
[5] a) G. A. Lawrance, M. Maeder, M. Napitupulu, A. L. Nolan, M. Rossignoli, V. Tiwow, P. Turner, *Inorg. Chim. Acta* **2005**, *358*, 3227–3235; b) R. B. Firestone, in *Table of isotopes* (Eds V. S. Shirley) 8th edition, John Wiley and Sons, Inc, New York, **1996**, 846–847; c) R. A. Fawwaz, W. Hemphill, H. S. Winchell, *J. Nucl. Med.* **1971**, *12*, 231–236.
[6] a) J. Van Rooyen, Z. Szucs, J. R. Zeevaart, *Appl. Radiat. Isot.* **2008**, *66*, 1346–1349; b) D. Filosofov, E. Kurakina, V. Radchenko, *Nucl. Med. Biol.* **2021**, *94–95*, 1–19; c) M. B. Idrissou, A. Pichard, B. Tee, T. Kibedi, S. Poty, J.-P. Pouget, *Pharmaceutica* **2021**, *13*, 980.
[7] Z. Chunfu, W. Yongxian, Z. Yongping, Z. Xiuli, *Appl. Radiat. Isot.* **2001**, 441–445.
[8] T. Das, S. Chakraborty, H. D. Sarma, S. Barnejee, *Radiochim. Acta* **2008**, *96*, 427–433.
[9] T. J. Wadas, E. H. Wong, G. R. Weisman, C. J. Anderson, *Chem. Rev.* **2010**, *110* (5), 2858–2902.
[10] E. W. Price, C. Orvig, *Chem. Soc. Rev.* **2014**, *43*, 260–290.
[11] a) D. Sarko, M. Eisenhut, U. Haberkorn, W. Mier, *Curr. Med. Chem.* **2012**, *19*, 2667–2688; b) D. Vivier, S. K. Sharma, B. M. Zeglis, *J. Label Compd. Radiopharm.* **2018**, *61*, 672–692; c) M. D. Bartholomä, *Inorg. Chim. Acta.* **2012**, *389*, 36–51; d) E. Lelong, J.-M. Suh, G. Kim, D. Esteban-Gómez, M. Cordier, M. H. Lim, R. Delgado, G. Royal, C. Platas-Iglesias, H. Bernard, R. Tripier, *Inorg. Chem.* **2021**, *60*, 15, 10857–10872; e) N. Camus, Z. Halime, N. Le Bris, H. Bernard, M. Beyler, C. Platas-Iglesias, R. Tripier, *RSC Adv.* **2015**, *5*, 85898–85910.
[12] a) E. Boros, A. B. Packard, *Chem. Rev.* **2019**, *119*, 870–901; b) T. Kostelnik, C. Orvig, *Chem. Rev.* **2019**, *119*, 2, 902–956.
[13] J. Funkhouser, *Curr. Drug Discov.* **2002**, *2*, 17–19.
[14] a) R. A. Werner, C. Bluemel, M. S. Allen-Auerbach, T. Higuchi, K. Herrmann, *Ann. Nucl. Med.* **2015**, *29*, 1–7; b) J. R. Ballinger, *Br. J. Radiol.* **2018**, *91* (1091), 20170969.
[15] a) D. Bailey, G. Schembri, K. Willowson, A. Hedt, E. Lengyelova, M. Harris., *J. Nucl. Med.* **2019**, *60* (supplement 1), 204; b) O. Keinänen, K. Fung, J. M. Brennan, N. Zia, M. Harris, E. van Dam, C. Biggin, A. Hedt, J. Stoner, P. S. Donelly, J. S. Lewis, B. M. Zeglis, *Proc. Natl. Acad. Sci. USA* **2020**, *117* (45), 28316–28327; c) J. M. Kelly, S. Ponnala, A. Amor-Coarasa, N. A. Zia, A. Nikolopoulou, C. Williams Jr., D. J. Schlyer, S. G. DiMagno, P. S. Donnelly, J. W. Babich, *Mol. Pharmaceutics* **2020**, *17* (6), 1954–1962.
[16] M. Rossignoli, C. C. Allen, T. W. Hambley, G. A. Lawrance, M. Maeder, *Inorg. Chem.* **1996**, *35*, 4961–4966.
[17] a) R. Wiesner, E. C. Lingafelter, *Inorg. Chem.* **1966**, *5*, 1770–1775; b) T. G. Appleton, J. R. Hall, *Inorg. Chem.* **1970**, *9*, 1800–1806.
[18] R. F. Fenske, D. S. Martin Jr, K. Ruedenberg, *Inorg. Chem.* **1962**, *1* (3), 441–452.
[19] A. R. Kapdi, I. J. S. Fairlamb, *Chem. Soc. Rev.* **2014**, *43*, 4751–4777.
[20] a) C. Bazzicalupi, A. Bencini, A. Bianchi, C. Giorgi, B. Valtancoli, *Coord. Chem. Rev.* **1999**, *184*, 243–270; b) C. De Stefano, A. Gianguzza, A. Pettignano, S. Sammartano, *J. Chem. Eng. Data* **2011**, *56*, 4759–4771.
[21] N. Le Bris, J. Pineau, L. M. P. Lima, R. Tripier, *Coord. Chem. Rev.* **2022**, *455*, 214343.
[22] a) R. M. Izatt, K. Pawlak, J. S. Bradshaw, *Chem. Rev.* **1995**, *95*, 2529–2586; b) R. Delgado, V. Félix, L. M. P. Lima, D. W. Price, *Dalton Trans.* **2007**, 2734–2745.
[23] J. M. Harrington, S. B. Jones, R. D. Hancock, *Inorg. Chim. Acta* **2005**, *358*, 4473–4480.

[24] a) L. M. P. Lima, D. Esteban-Gómez, R. Delgado, C. Platas-Iglesias, R. Tripier, *Inorg. Chem.* **2012**, 6916–6927; b) M. Frindel, N. Camus, A. Rauscher, M. Bourgeois, C. Alliot, L. Barré, J.-F. Gestin, R. Tripier, A. Faivre-Chauvet, *Nucl. Med. Biol.* **2014**, *41*, e49–e57.
[25] a) T. Le Bihan, A. S. Navarro, N. Le Bris, P. Le Saëc, S. Gouard, F. Haddad, J.-F. Gestin, M. Chérel, A. Faivre-Chauvet, R. Tripier, *Org. Biomol. Chem.* **2018**, *16*, 4261–4271; b) A. S. Navarro, T. Le Bihan, P. Le Saëc, N. Le Bris, C. Bailly, C. Saï-Maurel, J.-F. Gestin, M. Chérel, R. Tripier, A. Faivre-Chauvet, *Bioconjugate Chem.* 2**019**, 30, 9, 2393–2403.
[26] a) M. Yamashita, H. Ito, K. Toriumi, T. Ito, *Inorg. Chem.* **1983**, *10*, 1566–1568; b) K. Toriumi, M. Yamashita, H. Ito, T. Ito, *Acta Crystallogr.* **1986**, *C42*, 963–968.
[27] T. M. Hunter, S. J. Paisey, Hye-seo Park, L. Cleghorn, A. Parkin, S. Parsons, P. J. Sadler, *J. Inorg. Biochem.* **2004**, *98*, 713–719.
[28] B. Bosnich, C. K. Poon, M. L. Tobe, *Inorg. Chem.* **1965**, 1102–1108.
[29] Y. Dong, L. F. Lindoy, P. Turner, *Aust. J. Chem.* **2005**, *58*, 339–344.
[30] R. W. Hay, M. P. Pujari, W. T. Moodie, S. Craig, D. T. Richens, A. Perotti, L. Ungaretti, *J. Chem. Soc. Dalton Trans.* **1987**, 2605–2613.
[31] R. D. Hancock, R. J. Motekaitis, J. Mashishi, I. Cukrowski, J. H. Reibenspies, *J. Chem. Soc. Perkin Trans. 2* **1996**, 1925–1929; *Angew. Chem.* **2020**, *132*, 606–623.

Manuscript received: March 28, 2022
Accepted manuscript online: May 13, 2022
Version of record online: June 10, 2022